Available online at www.sciencedirect.com
SCIENCE DIRECT®
C. R. Mecanique 334 (2006) 105–110
COMPTES RENDUS MECANIQUE
http://france.elsevier.com/direct/CRAS2B/

Gravitational motion of a two-particle cluster between two parallel plane solid walls

Laurentiu Pasol, Antoine Sellier *

LadHyX, École polytechnique, 91128 Palaiseau cedex, France

Received 9 August 2005; accepted after revision 16 November 2005

Available online 22 December 2005

Presented by Évariste Sanchez-Palencia

Abstract

The slow viscous settling migration of a 2-particule cluster between two solid and parallel plane walls is investigated by resorting to a Boundary Element Method. The procedure, valid for arbitrarily-shaped bodies, is presented and preliminary numerical results for both identical spheres and a spheroid-sphere cluster are discussed. ***To cite this article: L. Pasol, A. Sellier, C. R. Mecanique 334 (2006).***

Résumé

Sédimentation de deux particules solides entre deux plans parallèles. On détermine la vitesse de sédimentation de deux particules solides dans un liquide confiné entre deux parois solides, planes et parallèles en négligeant les effets inertiels et en ayant recours à la seule résolution d'équations intégrales de frontière. Outre la théorie, des résultats numériques sont fournis pour la sédimentation de deux sphères identiques et d'une paire de particules comprenant un ellipsoide de révolution et une sphère. ***Pour citer cet article : L. Pasol, A. Sellier, C. R. Mecanique 334 (2006).***

Keywords: Fluid mechanics; Sedimentation; Two-particle cluster; Parallel walls; Boundary formulation

Mots-clés : Mécanique des fluides ; Sédimentation ; Paire de particules ; Parois parallèles ; Formulation intégrale

1. Introduction

We look at the slow viscous motion of two interacting solid particles settling in a liquid confined by two solid and parallel plane walls. For such boundaries, available approaches are unfortunately restricted to the case of one sphere [1–3], one particle [4] or two spheres [5] and a new procedure is therefore needed to handle the general case of two arbitrarily-shaped particles. The present Note advocates a fruitful and general treatment that permits us to compute the rigid-body motion of each particle at a reasonable CPU time cost and also gives preliminary results for two sphere–sphere and spheroid-sphere clusters.

* Corresponding author.
E-mail addresses: pasol@ladhyx.polytechnique.fr (L. Pasol), sellier@ladhyx.polytechnique.fr (A. Sellier).

1631-0721/$ – see front matter
doi:10.1016/j.crme.2005.11.007

2. Governing equations and advocated procedure

As illustrated in Fig. 1, we consider two solid particles $\mathcal{P}_n$ $(n = 1, 2)$ settling under the uniform gravity field $\mathbf{g}$ in a quiescent Newtonian liquid confined by the motionless planes Σ_1 $(x_3 = 0)$ and Σ_2 $(x_3 = H)$ with $H > 0$ the large enough gap with between the walls.

Since the arbitrarily-shaped solid $\mathcal{P}_n$ with surface S_n, volume $\mathcal{V}_n$ and mass $\mathcal{M}_n$ is not necessarily homogeneous we denote by O_n and O'_n it's center of volume and center of mass, respectively. Moreover, $\mathcal{P}_n$ experiences with respect to the walls a rigid-body motion with unknown translational velocity $\mathbf{U}^{(n)}$ (the velocity of O_n) and angular velocity $\mathbf{\Omega}^{(n)}$ whereas at each point M in the liquid domain Ω the fluid, with uniform viscosity μ and density ρ, has velocity $\mathbf{u}$, pressure $p + \rho\mathbf{g}.\mathbf{OM}$ and stress tensor $\boldsymbol{\sigma}$. Neglecting particles and fluid inertia, $(\mathbf{u}, p)$ is a quasi-static Stokes flow such that

$$\mu\nabla^2\mathbf{u} = \nabla p \quad \text{and} \quad \nabla.\mathbf{u} = 0 \quad \text{in } \Omega, \qquad (\mathbf{u}, p) \to (\mathbf{0}, 0) \quad \text{as } |\mathbf{OM}| \to \infty \tag{1}$$

$$\mathbf{u} = \mathbf{0} \quad \text{on } \Sigma = \Sigma_1 \cup \Sigma_2, \qquad \mathbf{u} = \mathbf{U}^{(n)} + \mathbf{\Omega}^{(n)} \wedge \mathbf{O_nM} \quad \text{on } S_n \text{ for } n = 1, 2 \tag{2}$$

Furthermore, on each surface S_n with unit outward normal $\mathbf{n}$ the requirement of zero net force and net torque (about O_n) supplements (1), (2) with the conditions

$$\mathbf{T}^{(n)} = \int_{S_n} \boldsymbol{\sigma}.\mathbf{n}\,\mathrm{d}S_n = (\rho\mathcal{V}_n - \mathcal{M}_n)\mathbf{g}, \qquad \mathbf{R}^{(n)} = \int_{S_n} \mathbf{O_nM} \wedge \boldsymbol{\sigma}.\mathbf{n}\,\mathrm{d}S_n = -\mathcal{M}_n\mathbf{O_nO'_n} \wedge \mathbf{g} \tag{3}$$

Using throughout Cartesian coordinates (O, x_1, x_2, x_3) and the usual tensor summation convention, we obtain the Cartesian velocity components $U_j^{(n)} = \mathbf{U}^{(n)}.\mathbf{e}_j$ and $\Omega_j^{(n)} = \mathbf{\Omega}^{(n)}.\mathbf{e}_j$ by extending the approach advocated in [6]. For $n = 1, 2$ and $i = 1, 2, 3$ we thus appeal to 12 Stokes flows $(\mathbf{u}_T^{(n),i}, p_T^{(n),i})$ and $(\mathbf{u}_R^{(n),i}, p_R^{(n),i})$ obeying (1) and the boundary conditions

$$\mathbf{u}_T^{(n),i} = \mathbf{u}_T^{(n),i} = \mathbf{0} \quad \text{on } \Sigma = \Sigma_1 \cup \Sigma_2, \qquad \mathbf{u}_T^{(n),i} = \delta_{nm}\mathbf{e}_i \quad \text{and} \quad \mathbf{u}_R^{(n),i} = \delta_{nm}\mathbf{e}_i \wedge \mathbf{O_nM} \quad \text{on } S_m \tag{4}$$

with δ_{mn} the Kronecker delta. For $L \in \{T, R\}$ the flow $(\mathbf{u}_L^{(n),i}, p_L^{(n),i})$ has stress tensor $\boldsymbol{\sigma}_L^{(n),i}$ and exerts on $S = S_1 \cup S_2$ the traction $\mathbf{f}_L^{(n),i} = \boldsymbol{\sigma}_L^{(n),i}.\mathbf{n}$. Recalling (3) and invoking the usual reciprocal identity [7] with the conditions (4) and $\mathbf{u} = \mathbf{0}$ on Σ yields, for $L \in \{T, R\}$,

$$\mathbf{L}^{(n)}.\mathbf{e}_i = \int_{S_n} \mathbf{u}_L^{(n),i}.\boldsymbol{\sigma}.\mathbf{n}\,\mathrm{d}S = \int_{S\cup\Sigma} \mathbf{u}_L^{(n),i}.\boldsymbol{\sigma}.\mathbf{n}\,\mathrm{d}S = \int_{S\cup\Sigma} \mathbf{u}.\boldsymbol{\sigma}_L^{(n),i}.\mathbf{n}\,\mathrm{d}S = \int_S \mathbf{u}.\mathbf{f}_L^{(n),i}\,\mathrm{d}S \tag{5}$$

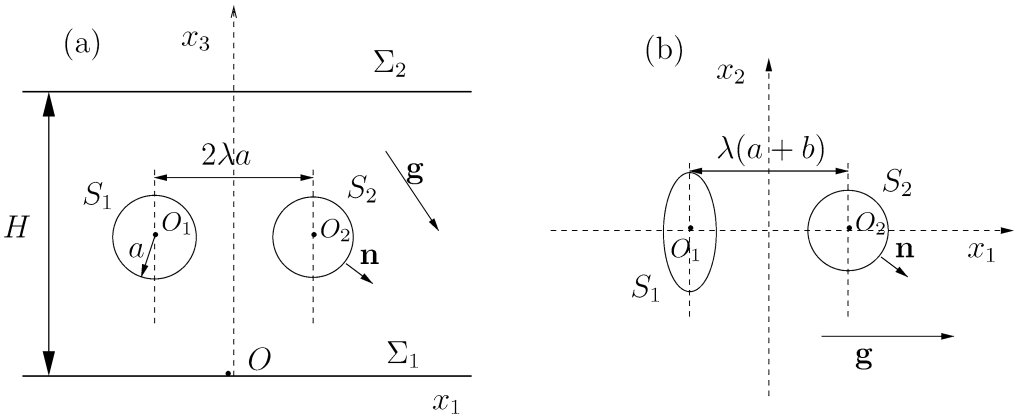

Fig. 1. A two-particle cluster settling between two parallel solid, motionless and plane walls Σ_1 $(x_3 = 0)$ and Σ_2 $(x_3 = H)$ with $H > 0$. (a) Side view for two identical spheres. (b) Top view for a sphere and a spheroid.

Fig. 1. Deux particules solides en sédimentation entre deux plans solides fixes et parallèles Σ_1 $(x_3 = 0)$ et Σ_2 $(x_3 = H)$ avec $H > 0$. (a) Vue latérale pour deux sphères identiques. (b) Vue de dessus pour une sphère et un ellipsoide de révolution.

Substituting in the right-hand side of (5) the condition (2) for $\mathbf{u}$ on S and setting

$$A^{(n),i,j}_{(m),L} = -\int_{S_m} \mathbf{e}_j.\mathbf{f}^{(n),i}_L \,\mathrm{d}S_m \quad \text{and} \quad B^{(n),i,j}_{(m),L} = -\int_{S_m} (\mathbf{e}_j \wedge \mathbf{O_m M}).\mathbf{f}^{(n),i}_L \,\mathrm{d}S_m \tag{6}$$

one thus casts (3) into the following 12-equation ($i = 1, 2, 3$ and $n = 1, 2$) linear system

$$\big\{A^{(n),i,j}_{(m),T} U^{(m)}_j + B^{(n),i,j}_{(m),T} \Omega^{(m)}_j\big\}\mathbf{e}_i = (\mathcal{M}_n - \rho \mathcal{V}_n)\mathbf{g} \tag{7}$$

$$\big\{A^{(n),i,j}_{(m),R} U^{(m)}_j + B^{(n),i,j}_{(m),R} \Omega^{(m)}_j\big\}\mathbf{e}_i = -\mathcal{M}_n(\mathbf{g} \wedge \mathbf{O}'_\mathbf{n}\mathbf{O_n}) \tag{8}$$

The real-valued matrix of the above system is symmetric by virtue of the reciprocal identity (use (6)) and also found to be positive-definite by extending the proof established in [6] for a single wall. Thus, (7), (8) admits a unique solution $(\mathbf{U}^{(1)}, \mathbf{\Omega}^{(1)}, \mathbf{U}^{(2)}, \mathbf{\Omega}^{(2)})$ determined by computing on the cluster's surface S the tractions $\mathbf{f}^{(n),i}_T$ and $\mathbf{f}^{(n),i}_R$ for $n = 1, 2$ and $i = 1, 2, 3$. Fortunately, these quantities are governed by a boundary-integral equation on S. The trick makes use of a suitable second-rank Green's tensor $T_{kj}(M, P)\mathbf{e}_k \otimes \mathbf{e}_j$ for arbitrary pole P and observation point M such that the velocity $\mathbf{T}_j = T_{kj}(M, P)\mathbf{e}_k$ is associated with a pressure field p_j obeying, for $\mathbf{O}M = x_i\mathbf{e}_i$ and $\mathbf{OP} = y_i\mathbf{e}_i$, the Stokes problem

$$\mu\nabla^2\mathbf{T}_j = \nabla p_j - \delta_d(x_1 - y_1)\delta_d(x_2 - y_2)\delta_d(x_3 - y_3)\mathbf{e}_j \quad \text{and} \quad \nabla.\mathbf{T}_j = 0 \quad \text{in } \Omega \tag{9}$$

$$\mathbf{T}_j(M, P) = \mathbf{0} \quad \text{for } M \text{ on } \Sigma_1 \cup \Sigma_2, \qquad (\mathbf{T}_j, p_j) \to (\mathbf{0}, 0) \quad \text{as } |\mathbf{PM}| \to \infty \tag{10}$$

with δ_d the Dirac pseudo-function. Not only because both $\mathbf{u}^{(n),i}_L$ and $\mathbf{T}_j$ vanish on the walls Σ_1 and Σ_2 but also since $\mathbf{u}^{(n),i}_L$ turns out to be a rigid-body motion on each surface S_1 and S_2, one deduces [8] the following Fredholm boundary-integral equations of the first kind

$$\big[\mathbf{u}^{(n),i}_L.\mathbf{e}_j\big](M) = -\int_{\mathcal{S}} T_{jk}(M, P)\big[\mathbf{f}^{(n),i}_L(P).\mathbf{e}_k\big]\,\mathrm{d}S_P \quad \text{for } M \text{ on } S \tag{11}$$

In summary, the motion of the two-particle cluster is determined as follows:

(i) First, we obtain the tractions $\mathbf{f}^{(n),i}_L$ by solving 12 boundary-integral equations (11) for $L = T, R$; $n = 1, 2$ and $i = 1, 2, 3$.
(ii) We subsequently calculate the quantities $A^{(n),i,j}_{(m),L}$, $B^{(n),i,j}_{(m),L}$ and solve the linear system (7), (8) to obtain the rigid-body motions $(\mathbf{U}^{(1)}, \mathbf{\Omega}^{(1)})$ and $(\mathbf{U}^{(2)}, \mathbf{\Omega}^{(2)})$.

3. Numerical implementation

The weakly-singular integral equation (11) is treated by splitting T_{jk} into singular and regular terms. More precisely, one obtains the decomposition

$$T_{jk}(M, P) = \frac{1}{8\pi\mu}\big\{G_{jk}(M, P) + R_{jk}(M, P)\big\}, \quad G_{jk}(M, P) = \frac{\delta_{jk}}{PM} + \frac{[\mathbf{PM}.\mathbf{e}_j][\mathbf{PM}.\mathbf{e}_k]}{PM^3} \tag{12}$$

with G_{jk} the usual stokeslet component [8] prevailing in absence of boundaries and R_{jk} a regular function independent of μ. Very or rather cumbersome formulae are available for R_{jk} in [9] or [3], respectively. The present work appeals to the results given in [3] which, however, are unfortunately too long to be reproduced here. The decomposition (12) yields an accurate numerical discretization of (11) by using 6-node curved triangular and isoparametric boundary elements [10] on S. For a N_n-node mesh on S_n Eq. (11) thus becomes a $3(N_1 + N_2)$-equation linear system which is solved by Gaussian elimination.

4. Results and discussion

To our very best knowledge, only [5] copes with two particles between two plane walls. Moreover, [5] rests on a quite different multipole approach restricted by essence to spherical bodies and gives accurate numerical results

Table 1
Computed coefficients $c_i^{(1)}$ and $c_i^{(2)}$ using increasingly refined N_n-node meshes on each S_n for either very close ($\lambda = 1.1$) or close ($\lambda = 2$) equal spheres arranged as sketched in Fig. 1(a)

Tableau 1
Coefficients $c_i^{(1)}$ et $c_i^{(2)}$ pour deux sphères identiques disposées selon la Fig. 1(a). Les sphères sont très proches ($\lambda = 1.1$) ou proches ($\lambda = 2$) et plusieurs maillages à N_n noeuds sur chaque surface S_n sont utilisés

$N_1 = N_2$	λ	$c_1^{(1)}$	$c_2^{(1)}$	$c_3^{(1)}$	$c_1^{(2)}$	$c_2^{(2)}$	$c_3^{(2)}$
74	1.1	3.20	1.96	2.92	−1.83	−0.110	0.137
242	1.1	3.34	1.97	2.94	−1.98	−0.116	0.132
1058	1.1	3.35	1.98	2.95	−1.99	−0.117	0.132
[5]	1.1	3.35	1.98	2.95	−1.99	−0.117	0.132
74	2	1.92	1.87	2.79	−0.365	0.199	0.116
242	2	1.93	1.87	2.80	−0.367	0.200	0.117
1058	2	1.93	1.87	2.80	−0.368	0.200	0.117
[5]	2	1.93	1.87	2.80	−0.368	0.200	0.117

only for two equal spheres $\mathcal{P}_n$, with center O_n, radius a, $H = 4a$ and such that $\mathbf{OO}_1.\mathbf{e}_3 = \mathbf{OO}_2.\mathbf{e}_3 = 2a$. For such a geometry, sketched in Fig. 1(a), [5] actually provides (with no summation over indices i in (13)) the coefficients

$$c_i^{(n)} = -A_{(n),T}^{(1),i,i}/(6\pi a\mu) \tag{13}$$

for a few values of the sphere–sphere separation parameter $\lambda = O_1O_2/2a > 1$. Our method is benchmarked in Table 1 against these results either for very close ($\lambda = 1.1$) or close ($\lambda = 2$) spheres and several N_n-node meshes on S_n with $N_1 = N_2$.

It clearly appears that using 242 nodes on each sphere ascertains a quite sufficient relative accuracy of order of one percent for the selected sphere–sphere gaps. We thus take $N_1 = N_2 = 242$ in investigating the settling of this cluster for the small gap with $H = 2.4a$ and spheres having the same uniform density ρ_s. Symmetries show that if $\mathbf{g} = g\mathbf{e}_i \neq \mathbf{0}$ the velocity components

$$u_{i,j}^{(n)} = 9\mu U_j^{(n)}/\big[2a^2(\rho_s - \rho)g\big] \quad \text{and} \quad w_{i,j}^{(n)} = 9\mu\Omega_j^{(n)}/\big[2a^3(\rho_s - \rho)g\big], \tag{14}$$

here normalized by the settling velocity of a single sphere, are zero except $u_i = u_{i,i}^{(1)} = u_{i,i}^{(2)}$ for $i = 1, 2, 3$; $w_2 = w_{2,3}^{(1)} = -w_{2,3}^{(2)}$ $(i = 2)$ and $w_3 = w_{3,2}^{(1)} = -w_{3,2}^{(2)}$ $(i = 3)$. These quantities are plotted in Fig. 2 versus the sphere–sphere separation λ in absence of walls, for a single wall Σ_1 and for both walls Σ_1 and Σ_2.

By symmetry, the walls induce interactions of equal magnitude which, as seen in Fig. 2, preserve the hierarchy $u_1 > u_2 > u_3$, $w_3 > -w_2$ observed for a single wall and slow down the cluster more but not twice more than in this latter case. As for a single wall, each velocity tends to its asymptote faster than in absence of walls and $u_1, w_3, -w_2$ increase as spheres approach whereas u_3 is nearly constant, i.e., spheres ignore each other for $\mathbf{g} = g\mathbf{e}_3$. By contrast, as λ increases u_2 monotonically decreases for a single wall but first decreases and then slowly increases for our close walls ($H = 2.4a$). Thus, for $\mathbf{OO}_1.\mathbf{e}_3 = 1.2a$ and Σ_2 ($x_3 = H$) with $H \geqslant 2.4a$ there exists a critical spacing λ_c at which $u_2(\lambda_c) = u_2(\infty)$ with each sphere ignoring the other one.

Contrary to the multipole method [5], the present approach can deal with non-spherical particles. We illustrate this point by replacing the sphere $\mathcal{P}_1$ of the previous 2-sphere cluster with a prolate spheroid having, as depicted in Fig. 1(b), center O_1 with $\mathbf{O}_1\mathbf{O}_2$ parallel to $\mathbf{e}_1$ and semiaxes b in the directions $\mathbf{e}_1$ or $\mathbf{e}_3$ and $c > b$ in the direction $\mathbf{e}_2$. Looking at the sensitivity of both wall–particle and particle–particle interactions to the shapes of the bodies, we require the spheroid and the sphere to be equivalent when isolated, i.e., to experience the same settling velocity $\mathbf{U}_s = 2a^2(\rho_s - \rho)\mathbf{g}/9$ for $H \to \infty$ and $O_1O_2 \to \infty$. If $\mathcal{P}_1$ has the uniform density ρ_s and a prescribed ratio $t = c/b$ this occurs for $\mathbf{g}.\mathbf{e}_2 = 0$ if (see [7])

$$b = a\left\{\frac{3}{8}\left[\frac{t^2}{t^2-1} + \frac{2t^3 - 3t}{(t^2-1)^{3/2}}\log\big(t + \sqrt{t^2-1}\big)\right]\right\}^{-1/2} \tag{15}$$

We select $t = 3/2$, thus arriving at $b \sim 0.89a$ and $c \sim 1.34a$, and plot in Fig. 3 the non-zero normalized velocities $u_{1,1}^{(n)}, u_{3,3}^{(n)}$ and $w_{3,2}^{(n)}$ versus the new separation parameter $\lambda = O_1O_2/(a + b) > 1$ for strong wall–particle interactions with $H = 2.4a$.

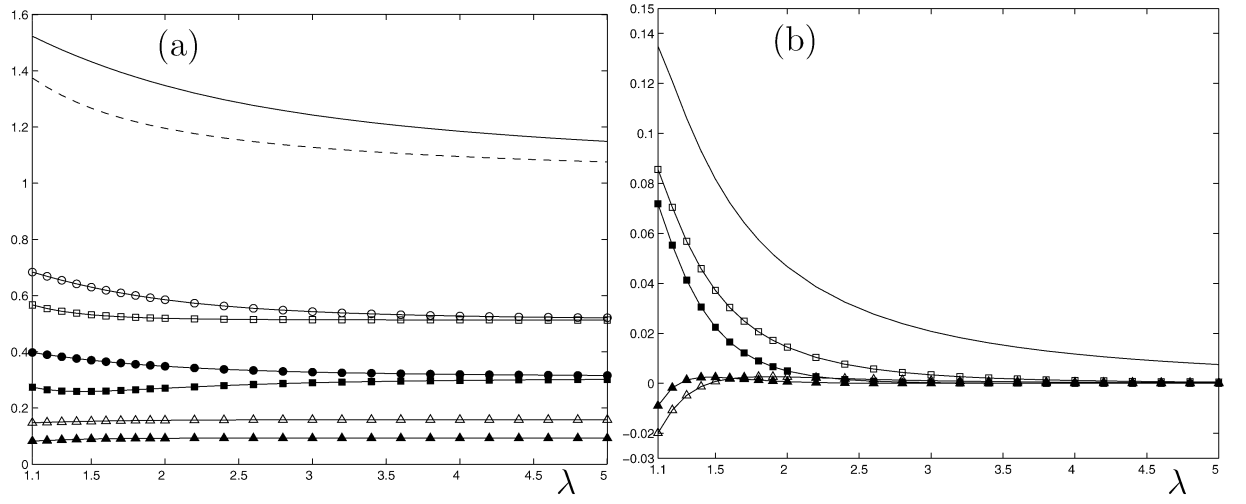

Fig. 2. Non-zero normalized translational and angular velocities for two identical spheres. (a) u_1 (solid curve) and $u_2 = u_3$ (dashed curve) in absence of walls; u_1 (○), u_2 (□) and u_3 (△) for a single wall Σ_1; u_1 (●), u_2 (■) and u_3 (▲) for two walls Σ_1 and Σ_2. (b) $w_3 = -w_2$ (solid curve) in absence of walls; w_2 (△) and w_3 (□) for a single wall Σ_1; w_2 (▲) and w_3 (■) for two walls Σ_1 and Σ_2.

Fig. 2. Vitesses non nulles adimensionnées de translation et de rotation pour deux sphères identiques. (a) u_1 (trait plein) et $u_2 = u_3$ (trait pointillé) en milieu infini ; u_1 (○), u_2 (□) et u_3 (△) en présence de la seule paroi Σ_1 ; u_1 (●), u_2 (■) et u_3 (▲) en présence de Σ_1 et Σ_2. (b) $w_3 = -w_2$ (trait plein) en milieu infini ; w_2 (△) et w_3 (□) en présence de la seule paroi Σ_1 ; w_2 (▲) et w_3 (■) en présence de Σ_1 et Σ_2.

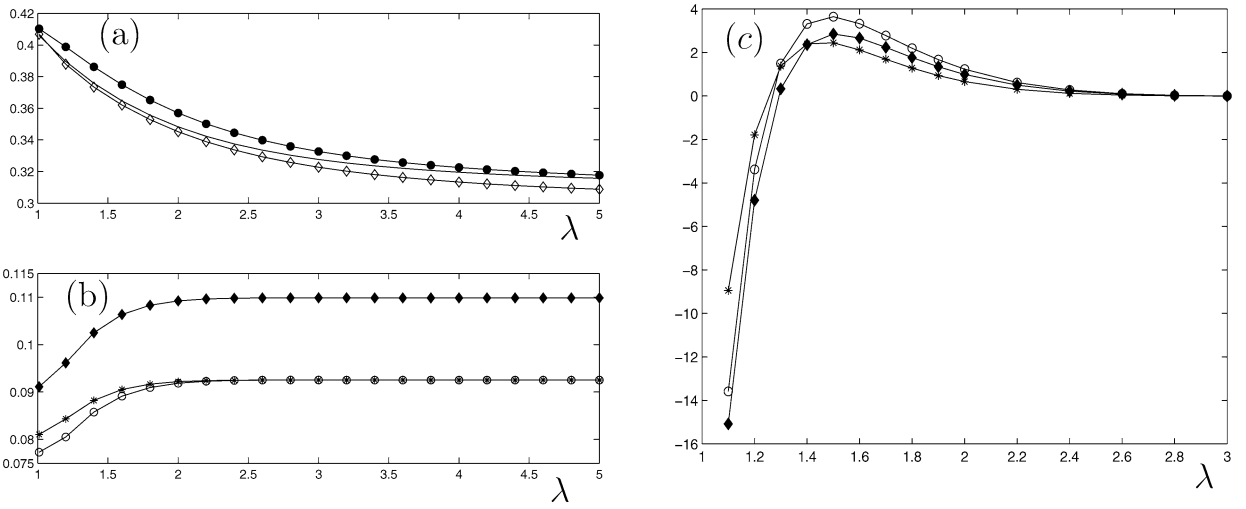

Fig. 3. Non-zero normalized velocities for a settling spheroid–sphere cluster. (a) Spheroid velocity $u_{1,1}^{(1)}$ (◇) and sphere velocity $u_{1,1}^{(2)}$ (●) for $\mathbf{g}$ parallel to $\mathbf{e}_1$ with $u_{1,1}^{(2)}$ for the 2-sphere cluster recalled by the solid curve. (b) Spheroid velocity $u_{3,3}^{(1)}$ (◆) and sphere velocity $u_{3,3}^{(2)}$ (○) for $\mathbf{g}$ parallel to $\mathbf{e}_3$ with $u_{3,3}^{(2)}$ (∗) for the 2-sphere cluster. (c) Quantities $10^3 w_{3,2}^{(1)}$ (◆) for the spheroid and $-10^3 w_{3,2}^{(2)}$ (○) for the sphere if $\mathbf{g}$ is parallel to $\mathbf{e}_3$ with the values of $10^3 w_{3,2}^{(1)} = -10^3 w_{3,2}^{(2)}$ (∗) for the 2-sphere cluster.

Fig. 3. Vitesses non nulles adimensionnées pour un ellipsoide de révolution et une sphère en sédimentation. (a) Vitesses $u_{1,1}^{(1)}$ (◇) de l'ellipsoide et $u_{1,1}^{(2)}$ (●) de la sphère si $\mathbf{g}$ est parallèle à $\mathbf{e}_1$, la valeur de $u_{1,1}^{(2)}$ pour deux sphères étant rappelée par la courbe en trait plein. (b) Vitesses $u_{3,3}^{(1)}$ (◆) de l'ellipsoide et $u_{3,3}^{(2)}$ (○) de la sphère si $\mathbf{g}$ est parallèle à $\mathbf{e}_3$ et rappel de $u_{3,3}^{(2)}$ (∗) pour deux sphères. (c) Quantités $10^3 w_{3,2}^{(1)}$ (◆) pour l'ellipsoide et $-10^3 w_{3,2}^{(2)}$ (●) pour la sphère si $\mathbf{g}$ est parallèle à $\mathbf{e}_3$ en rappelant la valeurs de $10^3 w_{3,2}^{(1)} = -10^3 w_{3,2}^{(2)}$ (∗) pour deux sphères.

As seen in Fig. 3(a), the sphere settles faster than the spheroid if $\mathbf{g}$ is parallel to $\mathbf{e}_1$ and the spheroid or the sphere translates slower or faster, respectively, than the 2-sphere cluster. In addition, the velocity of the 2-sphere cluster

tends to the velocity of the spheroid or the velocity of the sphere for close or distant spheroid and sphere, respectively. Fig. 3(b) reveals that, by contrast, the spheroid settles normal to the walls faster than the sphere (for distant particles, this agrees with a lubrification theory relevant for the addressed small wall–sphere and wall–spheroid gaps). In addition, the 2-sphere cluster moves this time faster than the sphere and slower than the spheroid even for very close particles. Finally, the spheroid and the sphere rotate, with $\mathbf{\Omega}^{(n)}$ parallel to $\mathbf{e}_2$, only when $\mathbf{g}$ is normal to the walls. As observed in Fig. 3(c), the sphere is found to rotate faster than the spheroid, except for very close particles ($\lambda \lesssim 1.2$).

5. Concluding remarks

Because (11) actually also holds in the entire fluid domain, the proposed procedure makes it possible to compute, if necessary, the velocity field $\mathbf{u}$ in the liquid. Finally, it should be outlined that our treatment is likely to be extended to the challenging case of clusters involving more than two arbitrarily-shaped and strongly interacting particles confined between two parallel solid plane walls. This basic issue however requires a substantial additional analysis which is therefore postponed to a future work.

References

[1] P. Ganatos, R. Pfeffer, S. Weinbaum, A strong interaction theory for the creeping motion of a sphere between plane parallel boundaries. 1. Perpendicular motion, J. Fluid Mech. 9 (1980) 739–753.
[2] P. Ganatos, R. Pfeffer, S. Weinbaum, A strong interaction theory for the creeping motion of a sphere between plane parallel boundaries. 2. Parallel motion, J. Fluid Mech. 9 (1980) 755–783.
[3] R.B. Jones, Spherical particle in Poiseuille flow between planar walls, J. Chem. Phys. 121 (1) (2004) 483–500.
[4] M.E. Staben, A.Z. Zinchenko, R.H. Davis, Motion of a particle between two parallel plane walls in low-Reynolds-number Poiseuille flow, Phys. Fluids 15 (6) (2003) 1711–1733.
[5] S. Bhattacharya, J. Blawzdziewicz, E. Wajnryb, Hydrodynamic interactions of spherical particles in suspensions confined between two planar walls, J. Fluid Mech. 541 (2005) 263–292.
[6] A. Sellier, Settling motion of interacting solid particles in the vicinity of a plane solid boundary, C. R. Mécanique 333 (5) (2005) 413–418.
[7] J. Happel, H. Brenner, Low Reynolds Number Hydrodynamics, Martinus Nijhoff, 1973.
[8] C. Pozrikidis, Boundary Integral and Singularity Methods for Linearized Viscous Flow, Cambridge Univ. Press, Cambridge, UK, 1992.
[9] N. Liron, S.M. Mochon, Stokes flow for a stokeslet between two parallel flat plates, J. Engrg. Math. 10 (1976) 287–303.
[10] M. Bonnet, Boundary Integral Equation Methods for Solids and Fluids, John Wiley & Sons Ltd, New York, 1999.